

Photophysical and anion sensing properties of platinum(II) terpyridyl complexes with phenolic ethynyl ligands†‡

Yang Fan,^a Yue-Mei Zhu,^a Feng-Rong Dai,^a Li-Yi Zhang^a and Zhong-Ning Chen^{*a,b}

Received 23rd May 2007, Accepted 19th July 2007

First published as an Advance Article on the web 1st August 2007

DOI: 10.1039/b707797a

A series of platinum(II) terpyridyl complexes with phenolic ethynyl ligands have been synthesized and characterized. Their photophysical and sensing properties towards anions such as fluoride, acetate and dihydrogenphosphate have been investigated. These complexes show a colorimetric response and fluorescence quenching in the presence of anions including fluoride, acetate and dihydrogenphosphate, and selective sensing towards fluoride in some cases. The sensing mechanism has been investigated by spectrophotometric and ¹H NMR titration.

Introduction

Platinum(II) terpyridyl-based complexes have shown attractive properties in the development of chemosensors, in which they usually serve as optical signaling centres.^{1–4} Taking advantage of the rich photophysical properties of platinum(II) terpyridyl systems,¹ a series of chemosensors with favourable sensing sensitivity to the corresponding analytes have been developed including selective labelling of biomolecules and detection of volatile organic compounds (VOCs).^{2,3} Recently, a series of Pt^{II} terpyridyl alkynyl complexes have been reported,⁴ which show colorimetric and enhanced fluorescence responses towards protons and cations including K⁺, Mg²⁺ and Ca²⁺ *etc.* In these complexes, the alkynyl ligands functionalized with amino, crown ether or azacrown ether are utilized as cation receptors, which are covalently bound to Pt^{II} terpyridyl signaling centres through Pt–acetylide σ -coordination. The binding of protons or cations to the receptors could induce optical signal switching between the LLCT (ligand-to-ligand charge transfer) and MLCT (metal-to-ligand charge transfer) excited states so as to afford the corresponding responses.

Aiming at exploring the optical responses of platinum(II) terpyridyl moieties towards anions, designed syntheses of a series of platinum(II) terpyridyl alkynyl complexes have been carried out in this group, in which acidic phenolic derivatives are employed as receptors. Due to the acidity of the phenolic hydroxyl, they can serve as receptors/binding sites for anions with basicity such as fluoride, acetate, and dihydrogenphosphate, inducing distinct responses to the platinum(II) terpyridyl signaling centres. Compared with numerous NH fragment-containing compounds such as ureas, thioureas, pyrroles and calix[4]pyrroles for anion sensing,⁵ only a few chemosensors utilizing hydroxyl OH containing phenolic or naphtholic derivatives as receptors have

been reported,⁶ in which organic chromophores/luminophores are usually employed as signaling centres. In this paper, we describe the syntheses, characterization, photophysical and sensing properties of a series of Pt^{II} terpyridyl complexes with phenolic ethynyl ligands (Chart 1), in which the Pt^{II} terpyridyl moiety serves as a signaling chromophore/luminophore and phenolic hydroxyl as a receptor/binding site for anions. These complexes undergo hydrogen-bonding interaction and/or proton transfer processes with anions during the recognition processes and demonstrate highly selective colorimetric sensing towards fluoride.

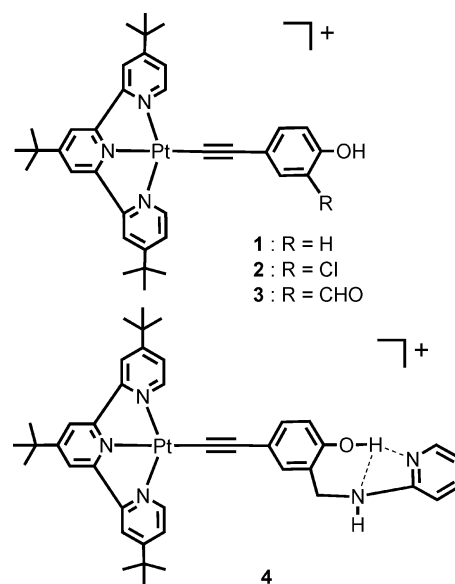


Chart 1

Results and discussion

Syntheses and characterisation

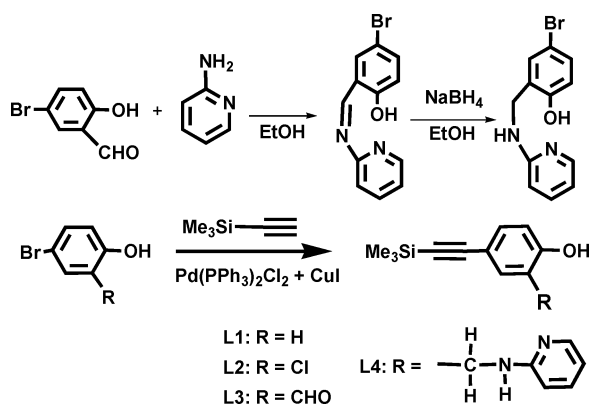
The synthetic routes to the phenolic alkynyl ligands are shown in Scheme 1. These alkynyl ligands **L1–L4** were synthesized by reaction of the corresponding bromo- or iodo-substituted ligands with (trimethylsilyl)acetylene through a Sonogashira coupling

^aState Key Laboratory of Structural Chemistry, Fujian Institute of Research on the Structure of Matter, Chinese Academy of Sciences, Fuzhou, Fujian, 350002, China. E-mail: czn@fjirsm.ac.cn; Fax: +86-591-8379-2346

^bState Key Laboratory of Organometallic Chemistry, Shanghai Institute of Organic Chemistry, Chinese Academy of Sciences, Shanghai, 200032, China

† CCDC reference number 648284. For crystallographic data in CIF or other electronic format see DOI: 10.1039/b707797a

‡ Electronic supplementary information (ESI) available: Fig. S1–S8 showing the spectrophotometric titration curves of **1–4** in the presence of various anions. See DOI: 10.1039/b707797a



Scheme 1 Synthetic routes to the phenolic ethynyl ligands.

reaction using $\text{Pd}(\text{PPh}_3)_2\text{Cl}_2\text{-CuI}$ as catalyst.^{8a} Platinum(II) terpyridyl alkynyl complexes **1–4** (Chart 1) were synthesized by modification of the literature methods.^{4c} All ligands **L1–L4** and platinum(II) complexes **1–4** have been characterized by elemental analyses, ESI-MS spectrometry, ¹H NMR and IR spectroscopy, and by X-ray crystallography for **3**.

In the ¹H NMR (DMSO-d_6) spectra of **1–4**, the phenolic OH proton signals are at 9.55, 10.35, 10.83 and 10.60 ppm, respectively. Compared with that in **1**, a downfield shift of the OH protons indicates the existence of an intramolecular hydrogen-bonding interaction O–H...Cl, O–H...O or O–H...N between phenolic OH and the *ortho*-substituent in **2–4**, as revealed in the crystal structure of **3**. Such an intramolecular hydrogen-bond would polarize the O–H bonds and create partial positive charge on the protons, inducing a de-shielding effect and a downfield shift of the OH proton.

An ORTEP drawing of the complex cation of **3** is depicted in Fig. 1. The Pt^{II} centre exhibits a distorted square-planar geometry built with a σ -coordinated C donor of acetylide and the tridentate chelating N₃ donors of terpyridyl. There exists an intramolecular hydrogen-bonding interaction between the phenolic O(1)–H(1A) and the *ortho* carbonyl oxygen O(2) with H(1A)...O(2) = 1.88 Å and O(1)–H(1A)...O(2) = 144.9°. The shortest Pt...Pt separation is 4.16 Å, suggesting the absence of Pt–Pt contacts in the crystal packing. Intermolecular π – π stacking between ^tBu₃tpy or phenyl rings is also unobserved.

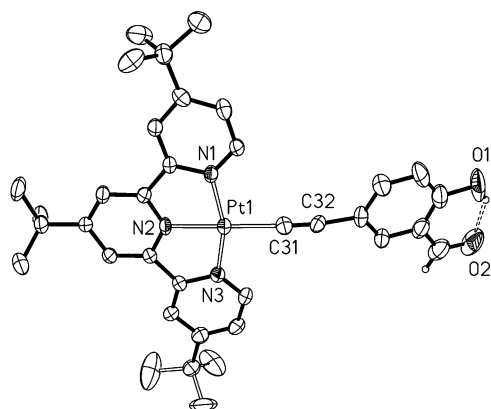


Fig. 1 ORTEP drawing of the cation of **3** with atom labeling scheme, showing 30% thermal ellipsoids.

Table 1 Electronic absorption and emission data for **1–4** in acetonitrile

Complex	$\lambda_{\text{abs}}/\text{nm}$ ($\epsilon/\text{dm}^3 \text{ mol}^{-1} \text{ cm}^{-1}$)	$\lambda_{\text{em}}^a/\text{nm}$	ϕ_{em}^b
1	257 (50245), 310 (17975), 404 (4230), 462 (5130)	633	0.0004
2	265 (48275), 309 (17970), 404 (4385), 443 (5290)	616	0.0038
3	245 (65770), 310 (16480), 378 (5420), 432 (4745)	608	0.0108
4^c	246 (74410), 309 (24425), 404 (4565), 470 (5290)		

^a In degassed dichloromethane at 298 K. ^b The emission quantum yields were measured in degassed dichloromethane solutions at 298 K and estimated relative to $[\text{Ru}(\text{bpy})_3]\text{Cl}_2$ in acetonitrile as the standard ($\phi_{\text{em}} = 0.062$). ^c **4** is non-emissive at 298 K.

Photophysical properties

The UV-vis electronic spectra of **1–4** in acetonitrile solutions show characteristic absorption bands of platinum(II) terpyridyl alkynyl complexes (Table 1),⁴ in which the absorption bands below 350 nm arise most probably from the intraligand (IL) transitions of the *tert*-butylterpyridyl and acetylide ligands. With reference to the spectroscopic assignments on a series of Pt^{II} terpyridyl alkynyl complexes described in the literature,⁴ the low-energy bands at *ca.* 350–430 and 430–570 nm are ascribed to $d\pi(\text{Pt}) \rightarrow \pi^*(^t\text{Bu}_3\text{tpy})$ MLCT (metal-to-ligand charge transfer) and $\pi(\text{C}\equiv\text{CC}_6\text{H}_3\text{R}(\text{OH})) \rightarrow \pi^*(^t\text{Bu}_3\text{tpy})$ LLCT (ligand-to-ligand charge-transfer) transitions, respectively. As shown in Fig. 2, the absorption bands of the LLCT transition of **1–4** are sensitive to the substituents on the phenolic ethynyl ligands. The low-energy absorption bands due to the LLCT transitions are 462, 443, 432 and 470 nm in **1–4**, respectively. Obviously, the LLCT absorption energy follows the order **4** < **1** < **2** < **3** which is readily interpreted in terms of the electronic effects of the substituents in the corresponding phenolic ethynyl ligands **L1–L4**. As the electron-withdrawing effects are H < Cl < CHO, the energy levels of the $\pi(\text{C}\equiv\text{CC}_6\text{H}_3\text{R}(\text{OH}))$ orbitals (HOMOs of LLCT transitions) in **1–3** are **1** > **2** > **3**, thus inducing a gradual increase of the HOMO–LUMO energy gap in the sequence **1** < **2** < **3**. As observed, the LLCT absorption is blue-shifted by 19 nm for **2** and 30 nm for **3** comparing with that of **1** (462 nm). For **4**, due to the minor electron-donating effect of the *ortho*-substituent $-\text{CH}_2\text{NHpy}$, the energy of the acetylide ligand-based HOMO is slightly raised compared with that of **1**, which consequently induces a minor red-shift of the LLCT absorption to 470 nm.

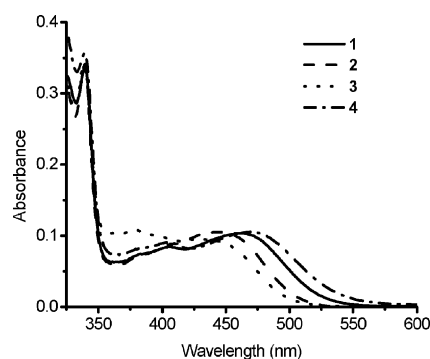


Fig. 2 UV-vis absorption spectra of **1–4** in acetonitrile solution.

Although **4** is non-emissive, **1–3** exhibit photoluminescence in degassed dichloromethane as indicated in Fig. 3. With reference to the previous luminescent studies on platinum(II) terpyridyl complexes, the emission state is tentatively assigned as a $d\pi(\text{Pt}) \rightarrow \pi^*({}^1\text{Bu}_3\text{tpy})$ ${}^3\text{MLCT}$ emission.^{1,4} As listed in Table 1, the emission maxima of **1–3** are centred at 633, 616 and 608 nm and the luminescent quantum yields in degassed dichloromethane are 0.0004, 0.0038 and 0.0108 for **1–3**, respectively. The changes in the emission energy for **1–3** accord well with the differences in electronic effects of the substituents. With an increase in the electron-withdrawing effect of the substituent ($\text{R} = \text{H}$ **1**, Cl **2**, CHO **3**) in the corresponding phenolic alkynyl ligands, the π -donating ability of the alkynyl ligands is weakened, which would lower the energy of the $d\pi(\text{Pt})$ -based HOMO.^{1c} Consequently, the energy of the ${}^3\text{MLCT}$ transition is raised and the emission is blue-shifted to higher energy. Interestingly, there are large variations in the emission quantum yields of **1–3** as shown in Fig. 3. For **1**, the low emission quantum yield of the ${}^3\text{MLCT}$ emission is likely a consequence of ${}^3\text{MLCT} \rightarrow {}^3\text{LLCT}$ interconversion and the consequent quenching through a ${}^3\text{LLCT}$ radiationless decay pathway.^{1c,4a,b} For **2**, the electron-withdrawing effect of the chloro group will lower the energy of the acetylide ligand-based HOMO, and the $d\pi(\text{Pt})$ -based HOMO is also lowered but to a lesser extent. Consequently, the ${}^3\text{LLCT}$ state is shifted to higher energies, and the ${}^3\text{MLCT} \rightarrow {}^3\text{LLCT}$ interconversion rate is decreased. As a result, the emission quantum yield of **2** is increased by 9.5 times compared with that of **1**. The stronger electron-withdrawing effect from $-\text{CHO}$ in **3** compared with that from chloro in **2** causes a further lowering in the acetylide ligand based HOMO energy and thus a diminished ${}^3\text{MLCT} \rightarrow {}^3\text{LLCT}$ emission quenching process, inducing a higher emission quantum yield for **3**, which is 27 times that of **1**.

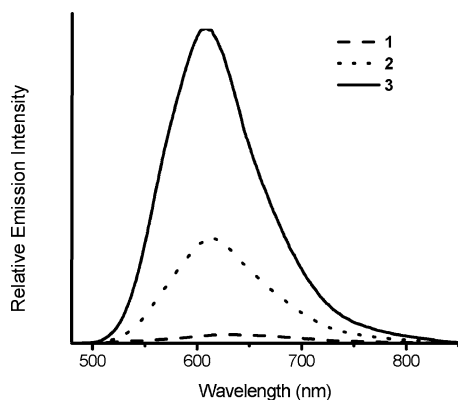


Fig. 3 Emission spectra ($\lambda_{\text{ex}} = 460$ nm) of **1–3** in degassed dichloromethane solution.

Colorimetric response to anions

The colorimetric response and sensing properties of **1–4** towards anions such as F^- , AcO^- and H_2PO_4^- (used as their tetra-*n*-butylammonium (TBA) salts) are investigated by spectrophotometric titration with standard solutions of the TBA salts of the anions in acetonitrile.

Fig. 4 shows the titration curves of **1** with tetra-*n*-butylammonium fluoride (TBAF). By addition of F^- from 0

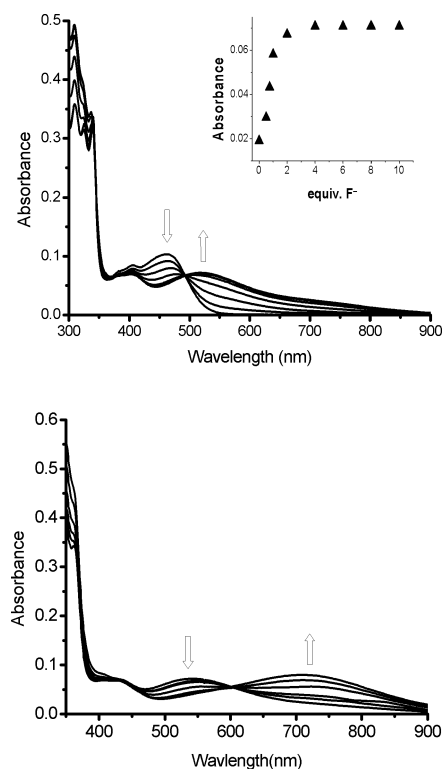


Fig. 4 UV-vis titration of an acetonitrile solution of **1** (2.0×10^{-5} M) with a standard solution of $[\text{Bu}_4\text{N}]\text{F}$ in acetonitrile. Top: addition of F^- from 0 to 2×10^{-4} M; inset: absorbance at 520 nm versus equivalents of F^- . Bottom: addition of F^- from 2×10^{-4} to 6×10^{-4} M.

to 10 equivalents, the absorption due to the LLCT transition at 463 nm decreases gradually, and red-shifts to 520 nm with progressively enhanced intensity. Well-defined isosbestic points are observed at 371 nm and 492 nm, indicating that only two absorbing species coexist in the equilibrium. The stoichiometric ratio of this new species is estimated to be $\text{F}^- : \mathbf{1} = 1 : 1$ from the titration profile of the band at 520 nm. By further addition of F^- from 10 to 30 equivalents, the LLCT band at 520 nm decreases progressively with the evolution of a new absorption band centred at 715 nm, originating from an intramolecular charge-transfer (ICT) transition of the deprotonated hydroxyl (phenolate) to the π -accepting terpyridyl ligand. As a result, the solution colour changes from yellow to blue, affording naked-eye colorimetric detection of F^- . The stepwise UV-vis spectral changes observed in the spectrophotometric titration suggest that the interaction of F^- with **1** is likely to operate in a two-step process.^{5e,g,j} At low concentrations of F^- , an $\text{O}-\text{H} \cdots \text{F}$ hydrogen-bonding interaction takes place between the phenol hydroxyl and F^- . Due to the strong hydrogen-bonding interaction, the negative charge on the donor is substantially increased and the $\text{O}-\text{H}$ bond is strongly polarized, which increases the electron density on the hydroxyl oxygen atom. Consequently, the energy of the phenolic ethynyl ligand based HOMO is raised, which induces a red-shift of the LLCT band to 520 nm. With further addition of F^- , a proton transfer process takes place from the hydroxyl to F^- . Upon deprotonation of the hydroxyl, the negative charge on the oxygen is partially delocalized from the phenolic ethynyl ligand to terpyridine through the Pt^{II} centre, so that the charge transfer process from the oxygen donor to the terpyridyl acceptor is highly

enhanced, causing the development of a ICT transition and a remarkable colour change. The corresponding spectrophotometric titration of **1** with AcO^- and H_2PO_4^- only show a smaller red-shift of the LLCT band to *ca.* 485 and 490 nm, respectively (Fig. S1, ESI ‡). Due to the lower basicity of AcO^- and H_2PO_4^- compared with F^- , they afford only a slight hydrogen-bonding interaction with the phenol hydroxyl, without the further proton transfer process.

The interaction of **1** with F^- is further investigated through ^1H NMR titration in DMSO-d_6 . As depicted in Fig. 5, upon addition of 5 equivalents of TBAF, the original OH proton signal at 9.55 ppm disappears, whereas a weak broad band appears at 16.06 ppm instead. Meanwhile, the proton signals of the phenyl show up-field shifts (*ca.* 0.18 ppm). With the further addition of 10 equivalents of TBAF, a distinct 1 : 2 : 1 triplet signal occurs at 16.13 ppm due to formation of $[\text{HF}_2]^-$.^{5d,j} At the same time, the phenyl proton signals show further up-field shifts (0.20 ppm for C(3)H and 0.58 ppm for C(2)H) because of the enhanced electron density on the phenyl ring upon deprotonation of the hydroxyl.^{5f,g,h} Hence, the stepwise changes in the ^1H NMR titration give further evidence of a two-step interaction process between **1** and F^- as suggested by the spectrophotometric titration. The disappearance of the OH proton signal together with the progressive occurrence of the $[\text{HF}_2]^-$ proton signal reveals unambiguously both O–H...F hydrogen bonding interaction and final proton transfer processes. The two-step interaction of **1** with F^- can thus be described by the equilibria^{5e} $\text{1-H} + \text{F}^- \leftrightarrow [\text{1-H}\cdots\text{F}^-]$ and $[\text{1-H}\cdots\text{F}^-] + \text{F}^- \leftrightarrow \text{1}^- + [\text{HF}_2]^-$.

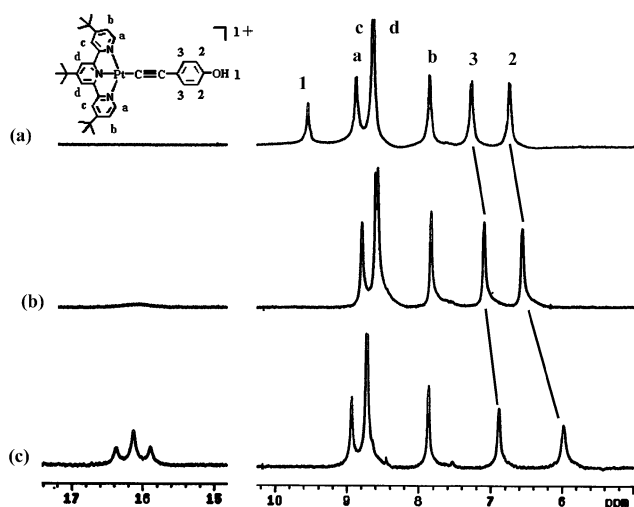


Fig. 5 ^1H NMR titration of **1** (1.0×10^{-2} M) in DMSO-d_6 with a standard solution of $[\text{Bu}_4\text{N}]\text{F}$ in DMSO-d_6 by addition of (a) 0, (b) 5, and (c) 10 equivalents of $[\text{Bu}_4\text{N}]\text{F}$.

In order to improve the colorimetric response to AcO^- and H_2PO_4^- , chloro (Cl) is introduced into the phenolic ligand in **2**. Because of the Cl electron-withdrawing nature in **2**, the acidity of the phenolic OH is increased, which would consequently enhance the binding affinity to AcO^- and H_2PO_4^- with less basicity relative to F^- . Remarkable colorimetric responses of **2** to F^- , AcO^- and H_2PO_4^- are observed, which changes from yellow to blue, light green and light orange, respectively. The hydrogen-bonding interaction and proton transfer process with the red-shift of the

LLCT band and the development of the ICT band centred at 655 nm are observed in titrations of **2** with F^- (Fig. S2, ESI ‡), AcO^- (Fig. S3, ESI ‡) and H_2PO_4^- (Fig. S4, ESI ‡), respectively. Due to the Cl electron-withdrawing effect, the energy of the acetylide ligand based HOMO of **2** is lower than that of **1** upon deprotonation by addition of excess anions, inducing an increase in the HOMO–LUMO gap and thus an ICT absorption with higher energy in **2** (Table 1).

Fig. 6 shows the titration curves of **3** with tetra-n-butylammonium fluoride (TBAF). Upon addition of F^- , the $d\pi(\text{Pt}) \rightarrow \pi^*(\text{Bu}_3\text{tpy})$ MLCT band at 378 nm is red-shifted to 428 nm with the absorption intensity increasing progressively. Meanwhile, the LLCT band centred at 475 nm decreases gradually in absorption intensity, and a new band centred at 600 nm occurs and increases gradually in intensity due to ICT mixed probably with some LLCT nature.^{4a,b} Variations of the MLCT and LLCT/ICT absorption energy in acetonitrile by addition of fluoride are reflected by an obvious colorimetric response from light yellow to cyan. Distinct isosbestic points occur at 344 nm, 378 nm and 475 nm (Fig. 6), indicating that two species coexist in the equilibrium. A stoichiometric ratio of the species formed by interaction of F^- with **3** is estimated to be 2 : 1 from the Job's plot (Fig. 6).^{5j}

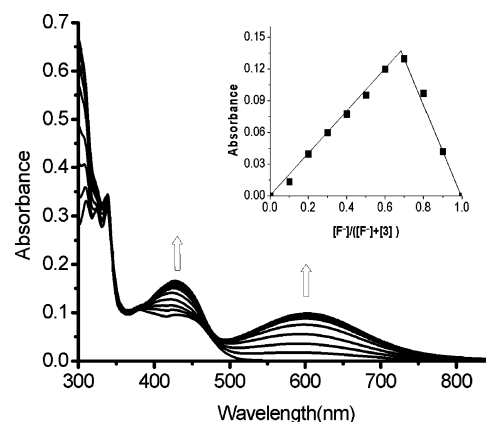


Fig. 6 UV-vis titration of **3** in acetonitrile solution (2.0×10^{-5} M) by addition of $[\text{Bu}_4\text{N}]\text{F}$ from 0 to 16.0×10^{-5} M; inset: Job's plot for F^- –**3** interactions. The total $[\text{F}^-] + [\text{3}] = 1.0 \times 10^{-4}$ M.

Titration of **3** with TBAF in DMSO-d_6 monitored by ^1H NMR spectroscopy affords distinct evidence of a fluoride-induced proton transfer process by deprotonation of the phenolic OH (Fig. 7). With addition of 2 equivalents of TBAF, the original signal of the phenolic OH proton at 10.82 ppm disappears whereas a new 1 : 2 : 1 triplet signal occurs at 16.13 ppm due to formation of $[\text{HF}_2]^-$.^{5d,j} Meanwhile, other proton signals in salicylaldehyde-5-acetylide show obvious up-field shifts (0.27–0.83 ppm) (Fig. 7) because of the enhanced electron density of the phenyl ring induced by deprotonation of the phenolic OH group. Accordingly, interaction of **3** with fluoride is undoubtedly a proton transfer process and can be described by the classical Brønsted acid–base equilibrium $\text{3-H} + 2\text{F}^- \leftrightarrow \text{3}^- + [\text{HF}_2]^-$.^{5e} The occurrence of such a neat proton transfer process without the prior intermolecular hydrogen-bonding interaction process seen for **1** or **2** is a direct consequence of the enhanced acidity in the phenolic OH group because of the presence of a strong electron-withdrawing

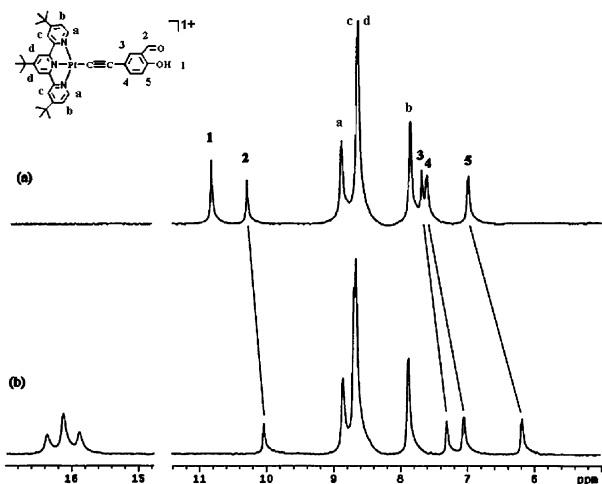


Fig. 7 ^1H NMR titration of **3** (1.0×10^{-2} M) in DMSO-d_6 with a standard solution of $[\text{Bu}_4\text{N}]\text{F}$ in DMSO-d_6 by addition of (a) 0 and (b) 2 equivalents of $[\text{Bu}_4\text{N}]\text{F}$.

ortho-CHO in **3**. Spectrophotometric titration of **3** with AcO^- (tetra-*n*-butylammonium acetate) results in similar red-shift of the MLCT and LLCT/ICT absorption (Fig. S5, ESI ‡). The corresponding titration, however, was not carried out with H_2PO_4^- due to the formation of a precipitate during the titration process.

Selective recognition of anions with similar basicity and surface charge density is a key issue in the development of colorimetric anion sensors.^{5m} Nevertheless, most of the anion sensors for F^- , AcO^- and H_2PO_4^- usually give similar colorimetric responses, which does not make discrimination between them easy.^{5o} Aiming at increasing the sensing selectivity for fluoride, 2-pyridinylaminomethyl ($-\text{CHNHC}_3\text{H}_4\text{N}$) is introduced to the *ortho*-position of the phenolic ligand in **4** (Chart 1), affording a 'pocket'-like binding site through formation of intramolecular hydrogen bonds $\text{O}-\text{H}\cdots\text{N}$ between the hydroxyl and pyridine/amine,^{6i,9} in which the hydrogen atom of the hydroxyl is significantly fastened and the intramolecular $\text{O}-\text{H}\cdots\text{N}$ hydrogen bond is not readily damaged by the addition of anions. As a consequence, only F^- which has the most electronegative nature can induce deprotonation of the hydroxyl in **4**. As shown in the titration curves (Fig. S6, ESI ‡) of **4** with F^- , distinct stepwise processes including formation of an $\text{O}-\text{H}\cdots\text{F}$ hydrogen-bond and proton transfer occur, inducing the appearance of a new ICT

band centred at 683 nm (Fig. 8) and dramatic colour changes from yellow to gray blue (Fig. 9). Corresponding titrations by addition of 50 equivalents of AcO^- (Fig. S7, ESI ‡) or H_2PO_4^- (Fig. S8, ESI ‡) only give a 10 nm red-shift of the LLCT absorption (Fig. 8). Therefore, through the elaborate design of the binding sites, high selectivity for F^- is achieved in **4** with a remarkable colorimetric response (Fig. 9).

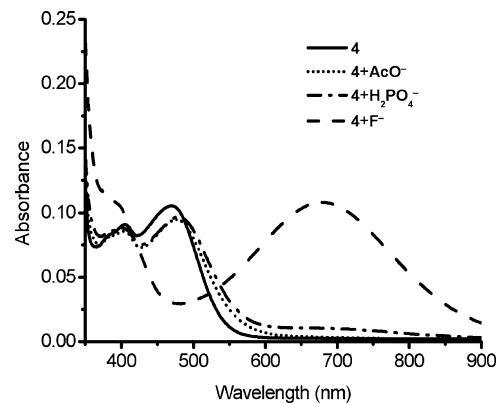


Fig. 8 UV-vis spectra changes of **4** in acetonitrile solution (2×10^{-5} M) after addition of 50 equivalents of anions.

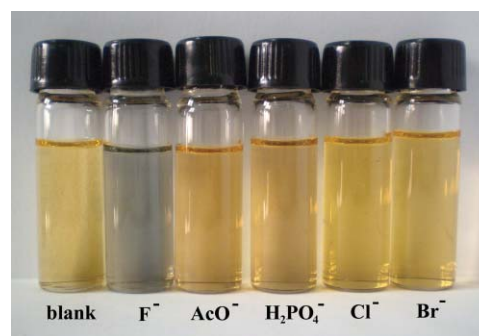


Fig. 9 Colour changes of **4** in acetonitrile solution (5.0×10^{-5} M) after addition of 10 equivalents of anions as TBA salts.

Binding constants of **1–4** with the anions, determined from spectrophotometric titration by nonlinear regression methods, are listed in Table 2.⁷ Titrations of **1–4** with Cl^- and Br^- show no detectable changes in the UV-vis spectra. As anticipated, the

Table 2 Binding constants and absorption maxima of **1–4** with anions in acetonitrile solution^a

Complex	$\log K^b$			LLCT/ICT $^{-1}$ /nm	
	F^-	AcO^-	H_2PO_4^-	Addition of F^-	
1	8.62 ± 0.29	4.23 ± 0.51	4.06 ± 0.32	462	716
2	4.53 ± 0.62				
	9.73 ± 0.43	4.93 ± 0.22	4.67 ± 0.19	443	655
3^c	6.56 ± 0.51	4.23 ± 0.35	4.12 ± 0.62		
	10.29 ± 0.36	6.37 ± 0.32		432	600
4^d	7.84 ± 0.56			470	683
	4.45 ± 0.68				

^a 2.0×10^{-5} M of complex in acetonitrile. ^b The binding constants to the anions were determined by nonlinear regression methods.⁷ ^c Titrations with H_2PO_4^- were not performed due to precipitate formation. ^d Minor spectral changes during titration with AcO^- or H_2PO_4^- were not suitable for accurate measurement of the binding constants.

colorimetric changes in the spectrophotometric titrations are fully reversible. With subsequent addition of a protic solvent such as methanol (competitive hydrogen bonding solvent), the reverse change in the spectra is observed and the solution colour gradually turns back, suggesting that the interaction between the complexes and the anions are hydrogen-bonding in nature.

Emission response to anions

The luminescent responses of **3** to F^- , AcO^- and $H_2PO_4^-$ were investigated by titration of **3** in dichloromethane solution with a standard solution of the TBA salts of the anions. Upon addition of 2 equivalents of F^- , the 3MLCT $d\pi(Pt) \rightarrow \pi^*(^tBu_3tpy)$ emission is quenched by ca. 87%, suggesting an emission “switch off” character (Fig. 10). Similar quenching is also observed by titration of **3** with AcO^- and $H_2PO_4^-$. It is suggested that anion-induced deprotonation of the hydroxyl group would increase the reduction potential of the phenolic ethynyl ligand and enhance the rate of electron transfer from the HOMO of the deprotonated phenolic ethynyl ligand to the platinum(II) terpyridyl excited states, thus inducing quenching or “switch off” of the emission. Similar emission responses to F^- , AcO^- and $H_2PO_4^-$ are observed for **2** in the titration experiments. The corresponding titrations for **1** and **4** did not perform owing to the low emission or non-emission of the 3MLCT state.

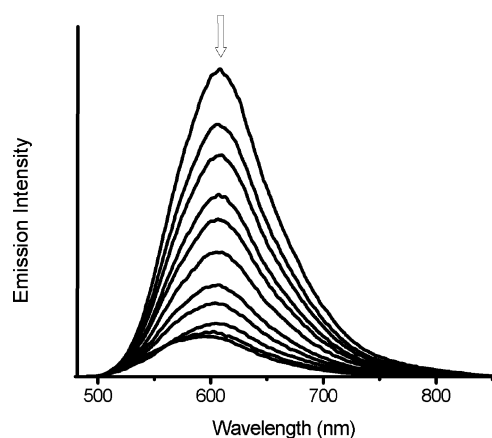


Fig. 10 The changes in fluorescent emission spectra ($\lambda_{ex} = 460$ nm) of **3** in dichloromethane solution (2.0×10^{-5} M) by addition of 0 to 2 equivalents of $[Bu_4N]F$.

Conclusions

We have demonstrated a rational strategy to design colorimetric sensing species for anions using a platinum(II) terpyridyl moiety as a signaling chromophore and a phenolic ethynyl ligand as a binding site. These complexes exhibit remarkable colorimetric responses and naked-eye detectable colour changes to anions such as F^- , AcO^- and $H_2PO_4^-$, in which **4** operates as a selective colorimetric sensor to F^- . The LLCT transition and 3MLCT emission are sensitive to the substituents at the *ortho*-position of the hydroxyl group, caused by electronic effects. The stepwise processes of the hydrogen-bonding interaction and the proton transfer take place in recognition of anions, inducing a significant red-shift of the LLCT absorption and development of a lower-

energy ICT transition. Through tuning binding affinity and elaborate design of the binding sites, selective sensing for F^- has been achieved. The fluoride-induced colorimetric response is caused by deprotonation of the phenolic OH group and consequently so is the enhanced intramolecular charge transfer from the phenolic alkynyl ligand to terpyridyl. Upon interactions of **1–4** with fluoride, the phenolic OH proton is released and the negative charge on the phenolic alkynyl ligand is significantly increased and delocalized to the platinum(II) terpyridyl moiety so that the charge transfer process from the phenolic oxygen donor to the terpyridyl acceptor is highly enhanced, consequently causing a naked-eye detectable colour response.

Experimental

General procedures

All synthetic manipulations were performed under an argon atmosphere using Schlenk techniques. The solvents were purified and distilled by standard procedures prior to use. The 4-iodophenol, 4-bromo-2-chlorophenol, 5-bromosalicylaldehyde, 2-aminopyridine and (trimethylsilyl)acetylene were commercially available (Alfa Aesar). 5-Trimethylsilylsalicylaldehyde (**L3**),^{8a} 4,4',4'-tri-*tert*-butyl-2,2',2''-terpyridine,^{8b} and $[Pt(^tBu_3tpy)Cl](PF_6)$ ^{1h} were synthesized by the literature methods.

Syntheses

4-Trimethylsilylethynylphenol (L1).^{8c} A mixture of 4-iodophenol (1.0 g, 4.55 mmol), (trimethylsilyl)acetylene (0.79 mL, 5.46 mmol), $Pd(PPh_3)_2Cl_2$ (160 mg, 0.23 mmol), and CuI (43 mg, 0.23 mmol) in Et_3N (50 mL) was stirred at 80 °C for 12 h under an argon atmosphere. After cooling to room temperature, the reaction mixture was filtered, and the filtrate was evaporated to dryness under reduced pressure to give an oily product. The crude product was purified by column chromatography on silica gel, using dichloromethane–methanol (100 : 2 v/v) as eluent. Yield 63%. Anal. calcd for $C_{11}H_{14}OSi$: C, 69.44; H, 7.42. Found: C, 69.51; H, 7.39%. ESI-MS: m/z 189.6 $[M - H]^-$. 1H NMR (DMSO- d_6): δ 9.90 (s, 1H, OH), 7.27 (d, 2H, $J = 8.0$ Hz, Ph), 6.74 (d, 2H, $J = 8.0$ Hz, Ph), 0.20 (s, 9H, CH_3). IR (KBr, ν/cm^{-1}): 2150 (s, $C\equiv C$).

2-Chloro-4-trimethylsilylethynylphenol (L2). The synthetic procedure was the same as that for **L1** except that 4-bromo-2-chlorophenol (1.0 g, 4.82 mmol) was used in place of 4-iodophenol. The crude product was purified by column chromatography on silica gel, using dichloromethane–methanol (100 : 2 v/v) as eluent. Yield 58%. Anal. calcd for $C_{11}H_{13}ClOSi$: C, 58.92; H, 5.85. Found: C, 58.85; H, 5.88%. ESI-MS: m/z 223.4 $[M - H]^-$. 1H NMR (DMSO- d_6): δ 10.73 (s, 1H, OH), 7.42 (d, 1H, $J = 2.0$ Hz, Ph), 7.25 (d, 1H, $J = 8.0$ Hz, Ph), 6.93 (d, 1H, $J = 8.0$ Hz, Ph), 0.20 (s, 9H, CH_3). IR (KBr, ν/cm^{-1}): 2150 (s, $C\equiv C$).

4-Bromo-2-(pyridin-2-ylaminomethyl)phenol. A mixture of 5-bromosalicylaldehyde (1.0 g, 4.97 mmol) and 2-aminopyridine (468 mg, 4.97 mmol) in ethanol (50 mL) was refluxed with stirring for 6 h under an argon atmosphere, excluding light. An orange precipitate formed during the reaction. After cooling to room temperature, $NaBH_4$ (940 mg, 24.85 mmol) was added in small portions with stirring. The orange precipitate gradually dissolved, and then the red solution turned colorless. After addition of H_2O

(50 mL), the solution was neutralized with AcOH (4 M) to pH = 7.0, followed by formation of a white precipitate. The mixture was filtered, and the collected white precipitate was washed with H₂O and EtOH, and dried under vacuum. Yield 75%. Anal. calcd for C₁₂H₁₁BrN₂O: C, 51.64; H, 3.97; N, 10.04. Found: C, 51.59; H, 3.95; N, 10.01%. ESI-MS: *m/z* 279.4 [M + H]⁺. ¹H NMR (DMSO-*d*₆): δ 10.62 (s, 1H, OH), 7.95 (d, 1H, *J* = 3.5 Hz, py) 7.40 (d, 1H, *J* = 7.0 Hz, Ph), 7.28 (d, 1H, *J* = 7.0 Hz, py), 7.21 (d, 1H, *J* = 7.0 Hz, Ph), 7.11 (s, 1H, NH), 6.75 (d, 1H, *J* = 8.0 Hz, Ph), 6.54 (d, 1H, *J* = 8.0 Hz, py), 6.51 (d, 1H, *J* = 5.5 Hz, py), 4.34 (d, 2H, *J* = 5.0 Hz, CH₂).

2-(Pyridin-2-ylaminomethyl)-4-trimethylsilylethynyl-phenol (L4). The synthetic procedure was the same as that for L1 except that 4-bromo-2-(pyridin-2-ylaminomethyl)phenol (1.0 g, 3.58 mmol) was used in place of 4-iodophenol. The crude product was purified by column chromatography on silica gel using dichloromethane as eluent. Yield 71%. Anal. calcd for C₁₇H₂₀N₂OSi: C, 68.88; H, 6.80; N, 9.45. Found: C, 68.79; H, 6.83; N, 9.49%. ESI-MS: *m/z* 297.3 [M + H]⁺. ¹H NMR (DMSO-*d*₆): δ 10.86 (s, 1H, OH), 7.94 (d, 1H, *J* = 3.5 Hz, py), 7.39 (d, 1H, *J* = 7.0 Hz, Ph), 7.25 (d, 1H, *J* = 7.0 Hz, py), 7.18 (d, 1H, *J* = 7.0 Hz, Ph), 7.09 (s, 1H, NH), 6.76 (d, 1H, *J* = 8.0 Hz, Ph), 6.55 (d, 1H, *J* = 8.0 Hz, py), 6.51 (d, 1H, *J* = 5.5 Hz, py), 4.33 (d, 2H, *J* = 5.0 Hz, CH₂), 0.18 (s, 9H, CH₃). IR (KBr, ν/cm⁻¹): 2150 s (C≡C).

[Pt(t-Bu₃tpy)(L1)](PF₆)(1). A mixture of [Pt(t-Bu₃tpy)Cl](PF₆) (200 mg, 0.26 mmol), 4-trimethylsilylethynylphenol (74 mg, 0.39 mmol), KF (45 mg, 0.78 mmol) and CuI (5 mg, 0.026 mmol) in a dichloromethane–methanol (2 : 1 v/v) solution was refluxed with stirring for 1 d under an argon atmosphere. The solvent was evaporated to dryness under reduced pressure, and the residue was extracted with dichloromethane. The crude product was purified by column chromatography on alumina using dichloromethane–methanol (100 : 2 v/v) as eluent. Yield: 73%. Anal. calcd for C₃₅H₄₀F₆N₃OPPt: C, 48.95; H, 4.69; N, 4.89. Found: C, 48.89; H, 4.73; N, 4.92%. ESI-MS: *m/z* 713.1 [M – PF₆]⁺. ¹H NMR (DMSO-*d*₆): δ 9.55 (s, 1H, OH), 8.89 (d, 2H, *J* = 6.5 Hz, tpy), 8.66 (s, 2H, tpy), 8.64 (s, 2H, tpy), 7.86 (d, 2H, *J* = 3.0 Hz, tpy), 7.28 (d, 2H, *J* = 8.0 Hz, Ph), 6.74 (d, 2H, *J* = 8.0 Hz, Ph), 1.52 (s, 9H, ¹Bu), 1.43 (s, 18H, ¹Bu). IR (KBr, ν/cm⁻¹): 2112 w (C≡C), 840 vs (PF₆).

[Pt(t-Bu₃tpy)(L2)](PF₆)(2). The synthetic procedure was the same as that for 1 except that 2-chloro-4-trimethylsilylethynylphenol (88 mg, 0.39 mmol) was used in place of 4-trimethylsilylethynylphenol. The crude product was purified by column chromatography on alumina, using dichloromethane–methanol (100 : 3 v/v) as eluent. Yield: 70%. Anal. calcd for C₃₅H₃₉ClF₆N₃OPPt: C, 47.06; H, 4.40, N, 4.70. Found: C, 47.12; H, 4.43, N, 4.65%. ESI-MS: *m/z* 747.1 [M – PF₆]⁺. ¹H NMR (DMSO-*d*₆): δ 10.35 (s, 1H, OH), 8.92 (d, 2H, *J* = 6.5 Hz, tpy), 8.67 (s, 2H, tpy), 8.65 (s, 2H, tpy), 7.85 (d, 2H, *J* = 3.0 Hz, tpy), 7.44 (s, 1H, Ph), 7.25 (d, 1H, *J* = 8.0 Hz, Ph), 6.94 (d, 1H, *J* = 8.0 Hz, Ph), 1.53 (s, 9H, ¹Bu), 1.44 (s, 18H, ¹Bu). IR (KBr, ν/cm⁻¹): 2115 w (C≡C), 840 vs (PF₆).

[Pt(t-Bu₃tpy)(L3)](PF₆)(3). The synthetic procedure was the same as that for 1 except that 5-trimethylsilylsalicylaldehyde (85 mg, 0.39 mmol) was used in place of 4-trimethylsilylethynylphenol. The crude product was purified by column chromatogra-

phy on silica gel using dichloromethane–methanol (100 : 1 v/v) as eluent. Yield 75%. Anal. calcd for C₃₆H₄₀O₂N₃PtPF₆: C, 48.76; H, 4.55; N, 4.74. Found: C, 48.70; H, 4.58; N, 4.72%. ESI-MS: *m/z* 741.0 [M – PF₆]⁺. ¹H NMR (DMSO-*d*₆): δ 10.83 (s, 1H, OH), 10.29 (s, 1H, O=CH), 8.88 (d, 2H, *J* = 6.5 Hz, tpy), 8.66 (s, 2H, tpy), 8.63 (s, 2H, tpy), 7.85 (d, 2H, *J* = 3.0 Hz, tpy), 7.68 (s, 1H, Ph), 7.60 (d, 1H, *J* = 6.5 Hz, Ph), 6.99 (d, 1H, *J* = 8.0 Hz, Ph), 1.53 (s, 9H, ¹Bu), 1.43 (s, 18H, ¹Bu). IR (KBr, ν/cm⁻¹): 2112 w (C≡C), 1650 vs (C=O), 840 vs (PF₆).

[Pt(t-Bu₃tpy)(L4)](PF₆)(4). The synthetic procedure was the same as that for 1 except that 2-(pyridin-2-ylaminomethyl)-4-trimethylsilylethynylphenol (116 mg, 0.39 mmol) was used in place of 4-trimethylsilylethynylphenol. The crude product was purified by column chromatography on silica gel using dichloromethane–methanol (100 : 1 v/v) as eluent. Yield 72%. Anal. calcd for C₄₁H₄₆F₆N₅OPPt: C, 51.04; H, 4.81; N, 7.26. Found: C, 51.11; H, 4.86; N, 7.23%. ESI-MS: *m/z* 818.9 [M – PF₆]⁺. ¹H NMR (DMSO-*d*₆): δ 10.60 (s, 1H, OH), 8.95 (d, 2H, *J* = 5.5 Hz, tpy), 8.71 (s, 2H, tpy), 8.69 (s, 2H, tpy), 7.97 (d, 2H, *J* = 3.0 Hz, tpy), 7.87 (d, 1H, *J* = 3.5 Hz, py), 7.42 (d, 1H, *J* = 7.0 Hz, Ph), 7.29 (d, 1H, *J* = 7.0 Hz, py), 7.20 (d, 1H, *J* = 6.5 Hz, Ph), 7.09 (s, 1H, NH), 6.77 (d, 1H, *J* = 8.0 Hz, Ph), 6.58 (d, 1H, *J* = 8.0 Hz, py), 6.52 (d, 1H, *J* = 5.5 Hz, py), 4.35 (d, 2H, *J* = 5.0 Hz, CH₂), 1.52 (s, 9H, ¹Bu), 1.43 (s, 18H, ¹Bu). IR (KBr, ν/cm⁻¹): 2112 w (C≡C), 840 vs (PF₆).

Physical measurements

Elemental analyses (C, H, N) were performed on a Perkin-Elmer model 240C automatic instrument. Electrospray ion mass spectra (ESI-MS) were recorded on a Finnigan LCQ mass spectrometer using dichloromethane–methanol as mobile phase. UV-vis absorption spectra were measured on a Perkin-Elmer Lambda 25 UV-Vis spectrometer. Infrared spectra were recorded on a magna 750 FT-IR spectrophotometer with KBr pellets. ¹H NMR spectra were measured on a Varian UNITY-500 spectrometer with SiMe₄ as the internal reference. Emission and excitation spectra were recorded on a Perkin-Elmer LS 55 Luminescence spectrometer with a red-sensitive photomultiplier type R928. Emission quantum yields were measured according to the method of Demas and Crosby.¹⁰ A degassed acetonitrile solution of [Ru(bpy)₃]Cl₂ (bpy = 2,2'-bipyridine) was used as the standard ($\Phi_{em} = 0.062$, excited at 436 nm).

Crystal structural determination

Crystals of 3 were obtained by diffusion of n-pentane into a 1,2-dichloroethane solution of 3. Single crystals sealed in capillaries with the mother-liquor were measured on a Rigaku SATURN70 CCD diffractometer using the ω scan technique at room temperature using graphite-monochromated Mo-K α ($\lambda = 0.71073$ Å) radiation. Absorption corrections by SADABS were applied to the intensity data. The structure was solved by direct methods, and the heavy atoms were located from an E-map. The remaining non-hydrogen atoms were determined from successive difference Fourier syntheses. All non-hydrogen atoms were refined anisotropically, and the hydrogen atoms were generated geometrically and refined with isotropic thermal parameters. The structure was refined on F^2 by full-matrix least-squares methods

using the SHELXTL-97 program package.¹¹ The disorder of the *tert*-butyl methyl group at C24 was refined as two partial-occupancy orientations and the C–C distances were refined with SADI restraints.

Acknowledgements

This work was supported financially by the NSFC (Grants 90401005, 20490210, 20521101 and 20625101), the 973 project (Grant 2007CB815304) from MSTC, the NSF of Fujian Province (Grant E0420002), and the fund from the Chinese Academy of Sciences (Grant KJCX2-YW-H01).

References

- (a) D. R. McMillin and J. J. Moore, *Coord. Chem. Rev.*, 2002, **229**, 113; (b) F. N. Castellano, I. E. Pomestchenko, E. Shikhova, F. Hua, M. L. Muro and N. Rajapakse, *Coord. Chem. Rev.*, 2006, **250**, 1819; (c) F. Guo and W. Sun, *Inorg. Chem.*, 2005, **44**, 4055; (d) J. F. Michalec, S. A. Bejune, D. G. Cuttall, G. C. Summerton, J. A. Gertenbach, J. S. Field, R. J. Haines and D. R. McMillin, *Inorg. Chem.*, 2001, **40**, 2193; (e) Q.-Z. Yang, L.-Z. Wu, Z.-X. Wu, L.-P. Zhang and C.-H. Tung, *Inorg. Chem.*, 2002, **41**, 5653; (f) V. W.-W. Yam, K. H.-Y. Chan, K. M.-C. Wong and N. Zhu, *Chem.–Eur. J.*, 2005, **11**, 4535; (g) M. G. Hill, J. A. Bailey, V. M. Miskowski and H. B. Gray, *Inorg. Chem.*, 1996, **35**, 4585; (h) S.-W. Lai, M. C. W. Chan, K.-K. Cheung and C.-M. Che, *Inorg. Chem.*, 1999, **38**, 4262; (i) V. W.-W. Yam, K. M.-C. Wong and N. Zhu, *J. Am. Chem. Soc.*, 2002, **124**, 6506; (j) E. Shikhova, E. O. Danilov, S. Kinayyigit, I. E. Pomestchenko, A. D. Tregubov, F. Camerel, P. Retailleau, R. Ziessel and F. N. Castellano, *Inorg. Chem.*, 2007, **46**, 3038.
- (a) K. W. Jennette, S. J. Lippard, G. A. Vassiliades and W. R. Bauer, *Proc. Natl. Acad. Sci., USA*, 1974, **71**, 3839; (b) S. J. Lippard, *Acc. Chem. Res.*, 1978, **11**, 211; (c) E. M. A. Ratilla, H. M. Brothers II and N. M. Kostic, *J. Am. Chem. Soc.*, 1987, **109**, 4592; (d) C. S. Peyratout, T. K. Aldridge, D. K. Crites and D. R. McMillin, *Inorg. Chem.*, 1995, **34**, 4484; (e) M. Cusumano, M. L. Di Pietro and A. Giannetto, *Inorg. Chem.*, 1999, **38**, 1754; (f) G. Arena, L. Monsu Scolaro, R. F. Pasternack and R. Romeo, *Inorg. Chem.*, 1995, **34**, 2994; (g) C. Yu, K. H.-Y. Chan, K. M.-C. Wong and V. W.-W. Yam, *Proc. Natl. Acad. Sci., USA*, 2006, **103**, 19652; (h) K. M.-C. Wong, W.-S. Tang, B. W.-K. Chu, N. Zhu and V. W.-W. Yam, *Organometallics*, 2004, **23**, 3459.
- T. J. Wadas, Q.-M. Wang, Y.-j. Kim, C. Flaschenreim, T. N. Blanton and R. Eisenberg, *J. Am. Chem. Soc.*, 2004, **126**, 16841.
- (a) K. M.-C. Wong, W.-S. Tang, X.-X. Lu, N. Zhu and V. W.-W. Yam, *Inorg. Chem.*, 2005, **44**, 1492; (b) X. Han, L.-Z. Wu, G. Si, J. Pan, Q.-Z. Yang, L.-P. Zhang and C.-H. Tung, *Chem.–Eur. J.*, 2007, **13**, 1231; (c) W.-S. Tang, X.-X. Lu, K. M.-C. Wong and V. W.-W. Yam, *J. Mater. Chem.*, 2005, **15**, 2714; (d) Q.-Z. Yang, L.-Z. Wu, H. Zhang, B. Chen, Z.-X. Wu, L.-P. Zhang and C.-H. Tung, *Inorg. Chem.*, 2004, **43**, 5195; (e) Q.-Z. Yang, Q.-X. Tong, L.-Z. Wu, Z.-X. Wu, L.-P. Zhang and C.-H. Tung, *Eur. J. Inorg. Chem.*, 2004, 1948; (f) K.-H. Wong, M. C.-W. Chan and C.-M. Che, *Chem.–Eur. J.*, 1999, **5**, 2845; (g) H.-S. Lo, S.-K. Yip, K. M.-C. Wong, N. Zhu and V. W.-W. Yam, *Organometallics*, 2006, **25**, 3537.
- (a) R. Martinez-Manez and F. Sancenon, *Chem. Rev.*, 2003, **103**, 4419; (b) P. D. Beer and P. A. Gale, *Angew. Chem., Int. Ed.*, 2001, **40**, 486; (c) A. P. de Silva, H. Q. Nimal Gunaratne, T. Gunnlaugsson, A. J. M. Huxley, C. P. McCoy, J. T. Rademacher and T. E. Rice, *Chem. Rev.*, 1997, **97**, 1515; (d) T. Gunnlaugsson, M. Glynn, G. M. Tocci, P. E. Kruger and F. M. Pfeffer, *Coord. Chem. Rev.*, 2006, **250**, 3094; (e) V. Amendola, D. E. Gomez, L. Fabbrizzi and M. Licchelli, *Acc. Chem. Res.*, 2006, **39**, 343; (f) V. Amendola, M. Boiocchi, L. Fabbrizzi and A. Palchetti, *Chem.–Eur. J.*, 2005, **11**, 120; (g) M. Boiocchi, L. Del Boca, D. E. Gomez, L. Fabbrizzi, M. Licchelli and E. Monzani, *J. Am. Chem. Soc.*, 2004, **126**, 16507; (h) M. Boiocchi, L. D. Boca, D. E. Gomez, L. Fabbrizzi, M. Licchelli and E. Monzani, *Chem.–Eur. J.*, 2005, **11**, 3097; (i) F. Han, Y. Bao, Z. Yang, T. M. Fyles, J. Zhao, X. Peng, J. Fan, Y. Wu and S. Sun, *Chem.–Eur. J.*, 2007, **13**, 2880; (j) Y. Wu, X. Peng, J. Fan, S. Gao, M. Tian, J. Zhao and S. Sun, *J. Org. Chem.*, 2007, **72**, 62; (k) C. B. Black, B. Andrioletti, A. C. Try, C. Ruiperez and J. L. Sessler, *J. Am. Chem. Soc.*, 1999, **121**, 10438; (l) T. Mizuno, W.-H. Wei, L. R. Eller and J. L. Sessler, *J. Am. Chem. Soc.*, 2002, **124**, 1134; (m) R. Nishiyabu, M. A. Palacios, W. Dehaen, Jr. and P. Anzenbacher, *J. Am. Chem. Soc.*, 2006, **128**, 11496; (n) T. Gunnlaugsson, P. E. Kruger, P. Jensen, J. Tierney, H. D. P. Ali and G. M. Hussey, *J. Org. Chem.*, 2005, **70**, 10875; (o) R. Nishiyabu, Jr. and P. Anzenbacher, *Org. Lett.*, 2006, **8**, 359.
- (a) T. Gareis, C. Huber, O. S. Wolfbeis and J. Daub, *Chem. Commun.*, 1997, 1717; (b) M. Baruah, W. Qin, N. Basaric, W. M. De Borggraeve and N. Boens, *J. Org. Chem.*, 2005, **70**, 4152; (c) K. M. Sun, C. K. McLaughlin, D. R. Lantero and R. A. Manderville, *J. Am. Chem. Soc.*, 2007, **129**, 1894; (d) D. H. Lee, K. H. Lee and J.-I. Hong, *Org. Lett.*, 2001, **3**, 5; (e) D. H. Lee, H. Y. Lee, K. H. Lee and J.-I. Hong, *Chem. Commun.*, 2001, 1188; (f) K. H. Lee, H.-Y. Lee, D. H. Lee and J.-I. Hong, *Tetrahedron Lett.*, 2001, **42**, 5447; (g) B.-G. Zhang, J. Xu, Y.-G. Zhao, C.-Y. Duan, X. Cao and Q.-J. Meng, *Dalton Trans.*, 2006, 1271; (h) Y.-G. Zhao, B.-G. Zhang, C.-Y. Duan, Z.-H. Lin and Q.-J. Meng, *New J. Chem.*, 2006, **30**, 1207; (i) X. Zhang, L. Guo, F.-Y. Wu and Y.-B. Jiang, *Org. Lett.*, 2003, **5**, 2667; (j) J.-S. Wu, J.-H. Zhou, P.-F. Wang, X.-H. Zhang and S.-K. Wu, *Org. Lett.*, 2005, **7**, 2133; (k) D. A. Jose, P. Kar, D. Koley, B. Ganguly, W. Thiel, H. N. Ghosh and A. Das, *Inorg. Chem.*, 2007, **46**, 5576.
- (a) B. Valeur, J. Pouget, J. Bourson, M. Kaschke and N. P. Ernstring, *J. Phys. Chem.*, 1992, **96**, 6545; (b) J. Bourson, J. Pouget and B. Valeur, *J. Phys. Chem.*, 1993, **97**, 4552.
- (a) K.-H. Chang, C.-C. Huang, Y.-H. Liu, Y.-H. Hu, P.-T. Chou and Y.-C. Lin, *Dalton Trans.*, 2004, 1731; (b) T. B. Hadda and H. L. Bozec, *Inorg. Chim. Acta*, 1993, **204**, 103; (c) E. Yashima, S. Huang, T. Matsushima and Yoshio Okamoto, *Macromolecules*, 1995, **28**, 4184.
- M. Suresh, D. A. Jose and A. Das, *Org. Lett.*, 2007, **9**, 441.
- J. N. Demas and G. A. Crosby, *J. Phys. Chem.*, 1971, **75**, 991.
- G. M. Sheldrick, *SHELXL-97, Program for the Refinement of Crystal Structures*, University of Göttingen, Göttingen, Germany, 1997.